Viser Technology Pte. Ltd.
Research and Application of Materials Science
DOI: 10.33142/rams.v4i2.8463

Research Article Open Access

Enhancement of Near-Field Radiative Heat Transfer based on High-Entropy Alloys

Shanshan DENG, Ping SONG*, Boxi ZHANG, Sen YAO, Zhixin JIN, Defeng GUO

State Key Laboratory of Metastable Materials Science and Technology and Key Laboratory for Microstructural Material Physics of Hebei Province, School of Science, Yanshan University, Qinhuangdao 066004, P. R. China

***Corresponding Author:** Ping Song,e-mail: psong@ysu.edu.cn*

Abstract:
The enhancement of near-field radiative heat transfer (NFRHT) has now become one of the research hotspots in the fields of thermal management and imaging due to its ability to improve the performance of near-field thermoelectric devices and near-field imaging systems. In this paper, we design three structures (multilayer structure, nanoporous structure, and nanorod structure) based on high-entropy alloys to realize the enhancement of NFRHT. By combining stochastic electrodynamics and Maxwell-Garnett's description of the effective medium, we calculate the radiative heat transfer under different parameters and find that the nanoporous structure has the largest enhancement effect on NFRHT. The near-field heat transfer factor (q) of this structure ($q = 1.40\times10^{9}$ W/ (m^2 K)) is three times higher than that of the plane structure ($q = 4.6\times10^{8}$ W/ (m^2 K)), and about two orders of magnitude higher than that of the SiO_2 plate. This result provides a fresh idea for the enhancement of NFRHT and will promote the application of high-entropy alloy materials in near-field heat radiation.

Keywords: *near-field radiative heat transfer; high-entropy alloys; multilayer structure; nanoporous structure; nanorod structure*

1 Introduction

Near-field radiative heat transfer (NFRHT) has become a hot topic in the fields of thermoptoelectronics [1-5], energy harvesting [6-8], sensing [9-10], and thermal management [11-13]. When the distance between two objects is at the nanometer level, the NFRHT can break the limit of Planck's law due to the coupling of photon tunneling and evanescent waves. This may be several orders of magnitude larger than the far-field heat transfer between two black bodies. To date, NFRHT has been studied in some isotropic and anisotropic materials. For isotropic materials, e. g., graphene, doped silicon, and gold, structures such as nanowires, nanopores, multilayer membranes, and 1D gratings have been designed to obtain a higher heat flow [14-21]. Graphene plasmons can couple evanescent waves in a near-field resonance, thereby enhancing the radiative heat flux through the nanoscale vacuum gap. Van Zwol et al. [14] demonstrated that the NFRHT between SiO_2 microspheres and the substrate was significantly increased by a single layer or several layers of graphene lying on the SiC substrate. Liu et al. [16] found that both doped silicon nanowires and nanopores can achieve an order of magnitude enhancement than bulk-doped silicon. Guerot et al. [21] predicted that the heat transfer between two gold gratings was increased by an order of magnitude more than that between two gold substrates. For anisotropic materials, the natural hyperbolic hexagonal boron nitride (hBN) has been mainly studied [22-24], which can support multiple orders of phonon-polaritonic waveguide modes in its two infrared bands. Surface plasmons in graphene can couple with the phonon polaritons in hBN films to form hybrid polaritons that greatly enhance photon tunneling and then enhance the NFRHT. Zhao et al. [22] found that monolayer graphene on hBN films is more than twice as heterogeneous as graphene monolayer or hBN films. Shi et al. [24] demonstrated that a multilayered structure consisting of five or more graphene-hBN units has a thermal flux four orders of magnitude larger than the black body.

Recently, we have studied the thermal radiation based on high-entropy alloys and found a broadband and wide-temperature-range thermal emission effect of high-entropy alloys [25]. This result predicts the possibility of applying high-entropy alloys to the field of NFRHT. In this paper, we combine hyperbolic materials hBN and high-entropy alloys to form multilayer metasurface structure and use high-entropy alloys to form nanoporous and nanorod structures. By changing the different parameters of the structure and materials, the optimal structure that maximizes the NFRHT efficiency is obtained. It is found that the nanoporous structure has the largest enhancement effect on NFRHT. The near-field heat transfer ability of this structure is two

Received on November 1, 2022; Accepted on December 11, 2022

orders of magnitude higher than the heat transfer rate of the SiO_2 plate under the same conditions.

2 Experiment

NiCrCuFeSi (referred to as NCCFS) high-entropy alloy is selected as the object to study NFRHT. To make the high-entropy alloy have better and more meaningful characteristics, we choose to use the nitrided NCCFS alloy (referred to as (NCCFS) N) for research and analysis [26]. The nitrogen content is determined by the nitrogen flow rate x.

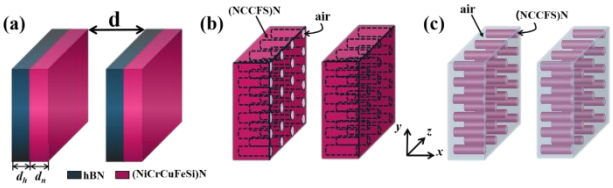

Figure 1 Schematic diagram of three structures based on the high-entropy alloys. (a) Multilayer structure. (b) Nanoporous structure. (c) Nanorod structure

We simulated the heat transfer factor under the optimal structure to explore the actual enhancement of NFRHT between parallel structures. Our first structure uses (NCCFS)N and hyperbolic hexagonal boron nitride (hBN) as materials to design a multilayer structure, as shown in Figure 1(a). Two flat plates are semi-infinite media, and d is the distance between two parallel plates. The thickness of the metal layer (NCCFS) N is expressed as d_n, and the thickness of the medium layer hBN is expressed as d_h. The dielectric function has a general expression in theory [27]:

$$\varepsilon(\omega)=1+\sum_j \frac{\omega_{p,j}^2}{\omega_{g,j}^2-\omega^2-2i\omega\gamma_j} \tag{1}$$

where ω is the frequency of the incident electromagnetic wave, $\omega_{p,j}$ the plasma frequency, $\omega_{g,j}$ the response frequency, γ_j the damping coefficient. The dielectric function model in this study is mainly the Drude model [28] applicable to metal materials. Its motion equation is:

$$m\ddot{x}+m\gamma\dot{x}=-eE_0\exp(-i\omega t) \tag{2}$$

where m is the electron mass and e is the charge and electric quantity. The real part (ε_1) and the imaginary part (ε_2) of the dielectric function can be deduced from the equation [16]. The expressions are:

$$\varepsilon_1(\omega)=1-\frac{\omega_p^2}{\omega^2+\gamma^2} \tag{3a}$$

$$\varepsilon_2(\omega)=1-\frac{\omega_p^2}{\omega^3+\gamma^2\omega} \tag{3b}$$

$$\omega_p^2=\frac{Ne^2}{m\varepsilon_0} \tag{3c}$$

In this paper, the real part and imaginary part of the dielectric function of (NCCFS) N high-entropy alloy at different nitrogen concentrations are from Ref. [26]. For multilayer parallel structures formed by alternate combination, $\varepsilon_x=\varepsilon_y=\varepsilon^{\parallel}$, $\varepsilon_z=\varepsilon^{\perp}$, its dielectric function formula is as follows [29]:

$$\varepsilon^{\perp}=\frac{\varepsilon_n d_n+\varepsilon_h d_h}{d_n d_h} \tag{4a}$$

$$\varepsilon^{\parallel}=\frac{d_n+d_h}{d_n/\varepsilon_n+d_h/\varepsilon_h} \tag{4b}$$

Our other two structures are the alternative combination of high-entropy alloy and air to form nanoporous or nanorod structures, as shown in Figure 1(b) and 1(c). In Maxwell – Garnett theory, the effective properties of composite media are obtained by taking one component of the composite as the substrate and embedding all other components into the substrate as filler materials. The materials do not contact each other. The relationship between dielectric functions in different directions and material parameters under nanoporous structure is as follows:

$$\frac{\varepsilon^{\parallel}-\varepsilon_a}{\varepsilon^{\parallel}+\varepsilon_a}=f\frac{\varepsilon_n-\varepsilon_a}{\varepsilon_n+\varepsilon_a} \tag{5a}$$

$$\varepsilon^{\perp}-\varepsilon_a=f(\varepsilon_n-\varepsilon_a) \tag{5b}$$

$$f_1=\frac{Vair}{V_{(NCCFS)N}} \tag{5c}$$

From the above formula, it can be deduced that the dielectric function expressions of the electric field parallel to the optical axis and perpendicular to the optical axis in the nanoporous structure are respectively:

$$\varepsilon^{\parallel}=\frac{2\varepsilon_a}{1-f_1\frac{\varepsilon_n-\varepsilon_a}{\varepsilon_n+\varepsilon_a}}-\varepsilon_a \tag{6a}$$

$$\varepsilon^{\perp}=f_1(\varepsilon_n-\varepsilon_a)+\varepsilon_a \tag{6b}$$

where f_1 refers to the volume filling rate of the nanoporous structure, which is equivalent to a controllable constant in the program, ε_n the dielectric function of the high entropy alloy, ε_a the dielectric constant of air, ε_z the dielectric function of the electric field along the optical axis. Because it is equivalent to the weighted average of the dielectric functions of (NCCFS) N film and air, it is essentially determined by a weakened Drude model.

For the nanorod structure, it is equivalent to the opposite of the nanoporous structure, that is, the columnar filling of the high-entropy alloy is carried out with air as the substrate. The dielectric function formula of nanorod structure is ε_n and ε_a after the position is changed, the filling ratio f_1 is the reciprocal of f_1. Biehs et al. calculated the heat transfer factor (q) between two anisotropic planar media separated by the true space gap d at the temperature T [30].

$$q=\frac{1}{8\pi^3}\int_0^{\infty}g(\omega,T)d\omega\int_0^{2\pi}\int_0^{\infty}\xi(\omega,\beta,\phi)\beta d\beta d\phi \tag{7a}$$

$$g(\omega,T)=\frac{\partial}{\partial T}\left(\frac{\hbar\omega}{e^{\hbar\omega/k_BT}-1}\right)=\frac{(\hbar\omega)^2e^{\hbar\omega/k_BT}}{k_BT^2(e^{\hbar\omega/k_BT}-1)^2} \tag{7b}$$

where the $\xi(\omega,\beta,\varphi)$ is the energy transmission coefficient. The heat transfer factor can directly reflect the efficiency of heat transfer. This paper discusses the enhancement of NFRHT by calculating the heat transfer factor.

3 Results and discussion

A. Enhancement of NFRHT by multilayer structure

The simulated result of the multilayer structure is shown in Figure 2(a). The value of q can be tuned by the distance between parallel plates (d) and the thickness ratio between (NCCFS)N film and Hbn (d_n/d_h). As shown in Figure 2(a), the value of q increases with the decrease of d and will have a sharp increase when d $<$ 30 nm. When changing the d_n/d_h, the value of q no longer varies monotonically as d_n/d_h changes. It's going to peak at a certain value of d_n/d_h. The maximum value of q is 3.84×10^8 W/ (m^2 K) at d_n/d_h = 0.1 when d = 30 nm. This result is 17.8% higher than that of a single Hbn film (q = 3.26×10^8 W/ (m^2 K)). We further investigate the nitrogen content (x) effect on q. As shown in Figure 2(b), with the increase of x, the value of q shows a trend of increasing first and then decreasing. When x = 1.0 sccm, the value of q reaches a peak of 4.64×10^8 W/ (m^2 K), which is 1.4 times higher than that of a single Hbn film.

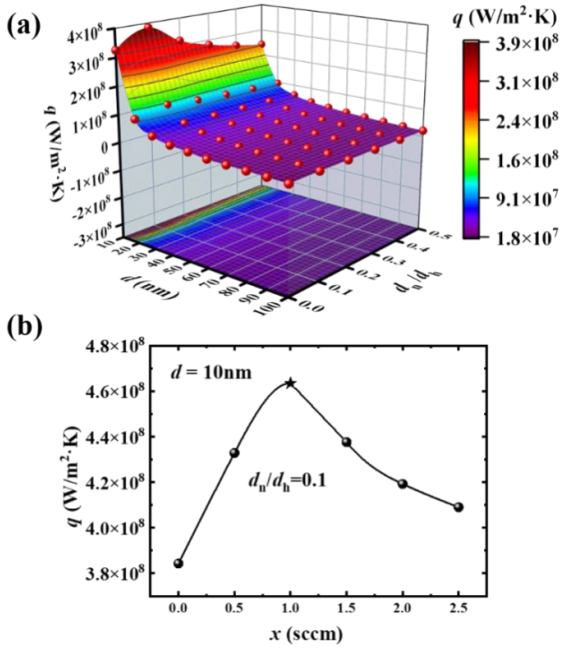

Figure 2 (a) q value of multilayer structure under different conditions. (b) The effect of nitrogen flow x on q under the condition of d = 10 nm and d_n/d_h = 0.1

B.Enhancement of NFRHT by nanoporous structure

To further increase the near-field heat transfer performance of high-entropy alloys, we designed the metastructure of the nanoporous structure. As shown in the inset of Figure 3, nanoporous (NCCFS)N materials are designed and the dimension scale of the nanoporous structure is defined by the volume filling ratio of air ($f_1 = V_{air}/V_{(NCCFS)N}$). The simulated values of q under different f_1 are shown in Figure3. When the distance (d) between the two nanoporous structures (as shown in Figure 1(b)) is fixed, the value of q increases gradually with the increase of f_1 and it reached 1.40×10^9 W/(m^2 K) at f_1 = 0.9. This result is about 20 times that of f_1 = 0 and is 2 orders of magnitude higher than the heat transfer rate of the SiO_2 plate under the same conditions. This may be due to the additional surface waves in the nanoporous structure generating supplementary heat transfer channels in the entire gap.

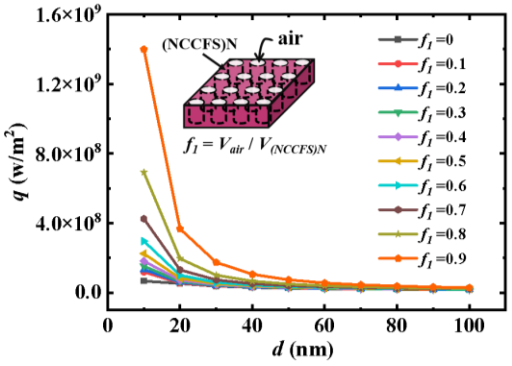

Figure 3 Distance between the two nanoporous structures (d) dependence of q under different f_1

C.Enhancement of NFRHT by nanorod structure

We also design the nanorod structure based on the (NCCFS)N high-entropy alloys and the dimension scale of the nanorod structure is defined by the volume filling ratio of the (NCCFS)N high-entropy alloys (as shown in the inset of Figure4). The simulated values of q under different f_2 are shown in Figure4. At the certain d value, the heat transfer factor of the nanorod structure decreases with the increase of f_2. The maximum value of q is 7.70×10^8W/ (m^2 K) at f_2 = 0.1 and d= 10 nm and this value of q is about 11 times that of f_2 = 1.

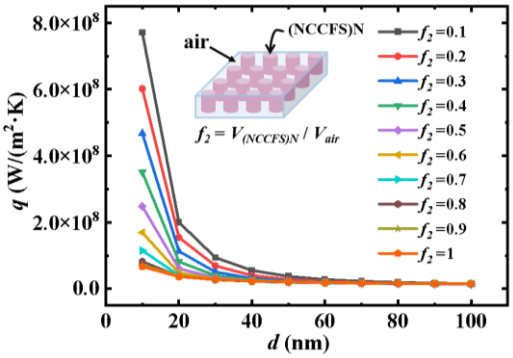

Figure 4 Distance between the two nanorod structures (d) dependence of q under different f_2

4 Conclusion

In summary, we calculated the heat transfer factors of multilayer structure, nanoporous, and nanorod structures designed based on (NCCFS) N high-entropy alloys under different parameters. The simulation results show that these three types of structures can effectively enhance near-field heat radiation. From the comparison of three structures and different material parameters, the nanoporous structure is the optimal structure for near-field heat transfer enhancement. The maximum q value is taken when d = 10 nm, f_1 = 0.9, and q = 1.40×10^9W/ (m^2 K), which is about 20 times that of f_1 = 0 and is 2 orders of magnitude higher than the heat transfer rate of the SiO_2 plate under the same conditions.

This may be due to the existence of additional surface waves in the nanoporous structure, which generates supplementary heat transfer channels in the entire gap. Our result will promote the application of high-entropy alloys in energy collection and thermal management.

Acknowledgments

This work is supported by the National Natural Science Foundation of China (Grant Nos. 52101233, 51931007, and 52071279), the Hebei Natural Science Foundation (No. E2022203010), and the Innovation Capability Improvement Project of Hebei Province (No. 22567605H).

References

[1] A. Karalis, J.D. Joannopoulos. Transparent and 'opaque' conducting electrodes for ultra-thin highly-efficient near-field thermophotovoltaic cells ,Sci Rep [J]. 7(2017): 14046.

[2] A. Fiorino, L. Zhu, D. Thompson, et al.. Nanogap near-field thermophotovoltaics, Nat Nanotech [J]. 13(2018): 806-811.

[3] R. Vaillon, J.P. Pérez, C. Lucchesi, et al.. Micron-sized liquid nitrogen-cooled indium antimonide photovoltaic cell for near-field thermophotovoltaics, Opt. Express [J]. 27 (2019) A11.

[4] G.T. Papadakis, S. Buddhiraju, Z. Zhao, et al.. Broadening Near-field emission for performance enhancement in thermophotovoltaics, Nano Lett [J]. 20 (2020) 1654-1661.

[5] B. Zhao, K. Chen, S. Buddhiraju, et al.. High-performance near-field thermophotovoltaics for waste heat recovery, Nano Energy. 41 (2017):344-350.

[6] J.Y. Chang, Y. Yang, L. Wang. Tungsten nanowire based hyperbolic metamaterial emitters for near-field thermophotovoltaic applications, Int. J. Heat Mass Transfer [J]. 87 (2015):237-247.

[7] S.A. Biehs, M. Tschikin, R. Messina, et al.. Super-Planckian near-field thermal emission with phonon-polaritonic hyperbolic metamaterials, Appl Phys. Lett [J]. 102 (2013):131106.

[8] M.S. Mirmoosa, F. Rüting, I.S. Nefedov, et al.. Effective-medium model of wire metamaterials in the problems of radiative heat transfer, J. Appl. Phys [J]. 115 (2014) 234905.

[9] R. Schilling, H. Schütz, A.H. Ghadimi, et al.. Near-field integration of a SiN nanobeam and a SiO_2 microcavity for heisenberg-limited displacement sensing, Phys. Rev. Applied [J]. 5 (2016) 054019.

[10] R.I. Stantchev, D.B. Phillips, P. Hobson, et al.. Compressed sensing with near-field THz radiation , Optica [J]. 4 (2017) 989.

[11] Y. Yang, S. Basu, L. Wang, Radiation-based near-field thermal rectification with phase transition materials, Appl. Phys. Lett [J]. 103 (2013) 163101.

[12] Y. Yang, S. Basu, L. Wang, Vacuum thermal switch made of phase transition materials considering thin film and substrate effects, J. Quant. Spectrosc. Ra [J]. 158 (2015) 69-77.

[13] P. Ben-Abdallah, S.A. Biehs, Phase-change radiative thermal diode, Appl. Phys. Lett [J]. 103 (2013) 191907.

[14] P.J. van Zwol, S. Thiele, C. Berger, et al.. Nanoscale radiative heat flow due to surface plasmons in graphene and doped silicon, Phys. Rev. Lett [J]. 109 (2012) 264301.

[15] A.I. Volokitin, B.N.J. Persson, Near-field radiative heat transfer between closely spaced graphene and amorphous SiO_2, Phys. Rev. B [J]. 83 (2011) 241407.

[16] X.L. Liu, R.Z. Zhang, Z.M. Zhang, Near-field radiative heat transfer with doped-silicon nanostructured metamaterials, Int. J. Hate Mass Tran [J]. 73 (2014) 389–398.

[17] S. Basu, L. Wang, Near-field radiative heat transfer between doped silicon nanowire arrays, Appl. Phys. Lett [J]. 102 (2013) 053101.

[18] P. Song, Y. Wu, L. Wang, et al.. The investigation of thermal stability of Al/NbMoN/NbMoON/SiO_2 solar selective absorbing coating, Sol. Energy Mater Sol. Cells [J]. 171 (2017) 253–257.

[19] C.J. Fu, Z.M. Zhang, Nanoscale radiation heat transfer for silicon at different doping levels, Int. J. Heat Mass Tran [J]. 49 (2006) 1703–1718.

[20] A. Kittel, W. Müller-Hirsch, J. Parisi, S.A. Biehs, et al.. Near-field heat transfer in a scanning thermal microscope, Phys [J]. Rev. Lett. 95 (2005) 224301.

[21] R. Guérout, J. Lussange, F.S.S. Rosa, et al.. Enhanced radiative heat transfer between nanostructured gold plates, Phys Rev. B [J]. 85 (2012) 180301.

[22] B. Zhao, Z.M. Zhang, Enhanced photon tunneling by surface plasmon–phonon polaritons in graphene/hBN heterostructures, J. Heat Transfer [J]. 139 (2017) 022701.

[23] B. Zhao, B. Guizal, Z.M. Zhang, et al.. Near-field heat transfer between graphene/hBN multilayers, Phys Rev. B [J]. 95 (2017) 245437.

[24] K. Shi, F. Bao, S. He, Enhanced near-field thermal radiation based on multilayer graphene-hBN heterostructures, ACS Photonics [J]. 4 (2017) 971–978.

[25] P. Song, C. Wang, Y. Sun, et al.. Broadband and wide-temperature-range thermal emitter with super-hydrophobicity based on oxidized high-entropy film, ACS Appl Mater [J]. 12 (2020) 4123–4128.

[26] P. Song, C. Wang, J. Ren , et al.. Modulation of the cutoff wavelength in the spectra for solar selective absorbing coating based on high-entropy films., Int. J. Mine. Metall Mater [J]. 27 (2020) 1371–1378.

[27] M. Cardona, Modulation Spectroscopy, Academic Press, New York [D], 1969.

[28] P. Drude, The Theory of Optics, Dover Publications, New York [D], 1925.

[29] S. Basu, B.J. Lee, Z.M. Zhang, Near-field radiation calculated with an improved dielectric function model for doped silicon, J. Heat Transfer [J]. 132 (2010) 023302.

[30] K. Joulain, J.P. Mulet, F. Marquier, et al.. Surface electromagnetic waves thermally excited: Radiative heat transfer, coherence properties and Casimir forces revisited in the near field, Surf. Sci. Rep [J]. 57 (2005) 59–112.